Semimetal-to-Semimetal Charge Density Wave Transition in $1T$-$TiSe_2$

G. Li,[1] W. Z. Hu,[1] D. Qian,[2] D. Hsieh,[2] M. Z. Hasan,[2] E. Morosan,[3] R. J. Cava,[3] and N. L. Wang[1,*]

[1]*Beijing National Laboratory for Condensed Matter Physics, Institute of Physics, Chinese Academy of Sciences, Beijing 100080, People's Republic of China*

[2]*Department of Physics, Joseph Henry Laboratories of Physics, Princeton University, Princeton, New Jersey 08544, USA*

[3]*Department of Chemistry, Princeton University, Princeton, New Jersey 08540, USA*

(Received 6 February 2007; published 13 July 2007)

We report an infrared study on $1T$-$TiSe_2$, the parent compound of the newly discovered superconductor Cu_xTiSe_2. Previous studies of this compound have not conclusively resolved whether it is a semimetal or a semiconductor—information that is important in determining the origin of its unconventional charge density wave (CDW) transition. Here we present optical spectroscopy results that clearly reveal that the compound is metallic in both the high-temperature normal phase and the low-temperature CDW phase. The carrier scattering rate is dramatically different in the normal and CDW phases and the carrier density is found to change with temperature. We conclude that the observed properties can be explained within the scenario of an Overhauser-type CDW mechanism.

DOI: 10.1103/PhysRevLett.99.027404 PACS numbers: 78.20.−e, 71.30.+h, 71.35.−y, 72.80.Ga

Charge density waves (CDW) and superconductivity are two important collective phenomena in solids. There has been tremendous interest in the interplay between these two states in condensed matter physics. The recent discovery of superconductivity upon controlled intercalation of Cu into CDW-bearing $1T$-$TiSe_2$ [1] offers a good opportunity to study the transition between the two states. As a first step, understanding the parent compound $1T$-$TiSe_2$ is essential.

The CDW state in $1T$-$TiSe_2$ has been known for several decades, but remains poorly understood. It shows a lattice instability around 200 K, below which it enters into a commensurate CDW phase associated with a $(2 \times 2 \times 2)$ superlattice [2–4]. The electronic structure has been studied by band structure calculations [5] and angular resolved photoemission spectroscopy (ARPES) measurements [6–12]. At energies near E_F, $1T$-$TiSe_2$ is governed by two bands: a holelike Se $4p$ band close to the Γ point and a Ti $3d$ band around the L point. Because of the small energy differences involved, ARPES experiments have not unambiguously shown whether the compound is a *semiconductor* or a *semimetal* in either the normal or CDW states.

This issue is central to resolving the mechanism of the CDW phase transition, which remains problematic. Contrary to other $1T$-type transition metal dichalcogenides, the CDW transition in $1T$-$TiSe_2$ is not likely to originate from Fermi surface (FS) nesting or saddle-point singularities, as parallel FS sheets have neither been predicted [5] nor observed [6–13]. One picture for the driving force for CDW formation is exciton formation at low temperature. However, the available experimental results in support of this picture are controversial [7–11,14]. There exist several other proposals for the driving mechanism, including an indirect Jahn-Teller effect [10,15], but no conclusive agreement has been reached. In this Letter, we study the change of the electronic structure as a function of temperature by optical spectroscopy. Although there exist several optical studies on this compound, most of them were performed only at room temperature or in the high energy region (above ~0.5 eV) [2,16–20]. A detailed study to low energy has been lacking. We argue here that Overhauser's scenario for CDW formation due to electron-hole bound pairs offers the most likely explanation to account for all the observed features.

Single crystals with reflective flat surfaces were grown as previously described [21]. The DC resistivity was measured by a standard four probe technique in a quantum design physical property measurement system. Similar to the data reported earlier [12], the $\rho(T)$ curve, as displayed in the inset of Fig. 1(a), shows a rather striking shape. The resistivity increases with decreasing T from 300 K and shows no distinct anomaly at the CDW transition near 200 K. After reaching a maximum near 150 K, it decreases on further cooling. This behavior is rarely seen in metallic or semiconducting compounds, and is also not seen in conventional CDW-bearing materials.

The frequency-dependent reflectance spectra $R(\omega)$ at different T were measured by a Bruker IFS 66 v/s spectrometer in the range from 50 to 25 000 cm^{-1} and a grating-type spectrometer from 20 000 to 50 000 cm^{-1}. The sample was mounted on an optically black cone on the cold finger of a He flow cryostat. An *in situ* gold (50–15 000 cm^{-1}) and aluminum (9000–50 000 cm^{-1}) overcoating technique was employed for reflectance measurements. A Kramers-Kronig transformation of $R(\omega)$ was used to obtain the other optical response functions. A Hagen-Rubens relation was used for low frequency extrapolation, and a constant extrapolation for high frequency to 300 000 cm^{-1} followed by an ω^{-2} function was used for the higher energy side.

Figure 1(a) shows the $R(\omega)$ spectra at different T over the frequency range from 50 to 6000 cm^{-1} and Fig. 1(b) shows the spectra in an expanded plot from 50 to

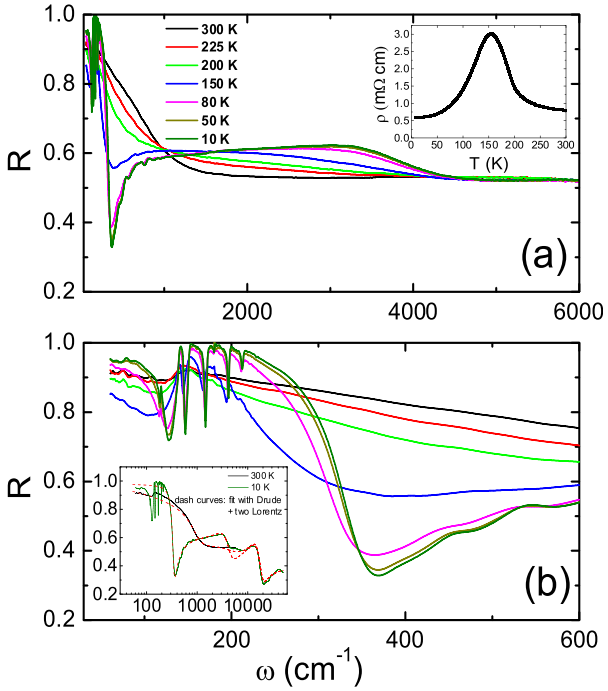

FIG. 1 (color online). (a) The temperature dependent $R(\omega)$ in the frequency range from 30 to 6000 cm^{-1}. The inset is the T-dependent DC resistivity. (b) The expanded plot of $R(\omega)$ from 30 to 600 cm^{-1}. The inset shows $R(\omega)$ data up to 50 000 cm^{-1} on a logarithm scale. Dash curves are fitted to a simple Drude-Lorentz model.

600 cm^{-1}. The inset shows the spectra over from 50 to 50 000 cm^{-1} on a logarithmic scale at two different temperatures. There is a very strong phonon structure near 130 cm^{-1} at both high and low temperatures. The antiresonance behavior of this phonon indicates strong coupling between electrons and the phonon. In the CDW phase below 200 K, several new phonon lines appear, evidencing the symmetry change of the structure.

Most importantly, the reflectance spectra show an unambiguously metallic character at both high and low T. The carrier damping rate is dramatically different in the normal and CDW phases. The $R(\omega)$ at high T displays a linear-ω dependence up to an edge of 1100 cm^{-1}. This is the well-known overdamped behavior, similar to the situation in high-T_c cuprates, indicating rather strong carrier scattering. With decreasing T, $R(\omega)$ at low ω decreases, leading to an edge shift towards the low energy region. At the same time, $R(\omega)$ between 1000 and 5000 cm^{-1} increases. When the sample is cooled below 150 K, a sharp, well-defined plasma edge appears and then shifts slightly to higher ω with decreasing T. The screened plasma edge frequency is located between 300–350 cm^{-1} (~40 meV) at low T, which is almost 2 orders of magnitude lower in frequency than for usual metals. The extremely low plasma edge frequency reveals a very small carrier density. Such a well-defined plasma edge is an indication of rather small carrier damping.

The formation of the plasma edge and its evolution with T can be seen more clearly from the energy loss function, $\mathrm{Im}[-1/\epsilon(\omega)]$, shown in Fig. 2. In the energy loss function, the peak position indicates the screened plasma frequency, while the peak width is related to the carrier damping rate. As T decreases from 300 to 150 K, the screened plasma frequency decreases from 1132 to 300 cm^{-1}, but it then increases from 300 to 347 cm^{-1} as the compound is cooled from 150 to 10 K. At the same time, the spectral shape changes from a broad feature to a sharp peak structure, suggesting a dramatic reduction of the carrier damping at low T. The peaklike feature near 4000 cm^{-1} is not the plasma edge, but is the interband transition due to the formation of a gap.

To quantitatively analyze the carrier density and damping, we fit the experimental reflectance to a simple Drude-Lorentz model:

$$\epsilon(\omega) = \epsilon_\infty - \frac{\omega_p^2}{\omega^2 + i\omega/\tau} + \sum_{i=1}^{2} \frac{S_i^2}{\omega_i^2 - \omega^2 - i\omega/\tau_i}. \quad (1)$$

This expression contains a Drude term and two Lorentz terms, which approximately capture the contributions by free carriers and interband transitions. As shown in the inset of Fig. 1(b), this simple model can reasonably reproduce the $R(\omega)$ curves: the calculated curves at 300 and 10 K are displayed. In the inset of Fig. 2, we plot the plasma frequency ω_p and scattering rate $1/\tau$ obtained for the Drude term as a function of T. Both parameters show a dramatic change in the temperature range of 150–200 K, in conjunction with the CDW phase transition. An $\epsilon_\infty = 19$ is obtained by fitting. (As the interband transitions are not our focus here, we do not show the parameters for the Lorentz terms.) From this approach, we obtain the unscreened plasma frequency $\omega_p \sim 8000$ cm^{-1} at 300 K, which gives a carrier density of 7.1×10^{20} $1/\mathrm{cm}^3$ if $m = m_e$ is assumed, which is in good agreement with band structure calculation [5]. At 10 K, the value of $\omega_p \sim 2700$ cm^{-1} implies a carrier density of 8.1×10^{19} $1/\mathrm{cm}^3$.

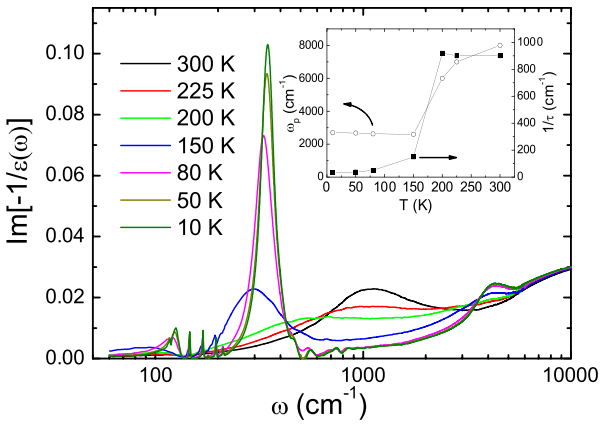

FIG. 2 (color online). The energy loss function spectra at different T. Inset: the variation of the plasma frequency and scattering rate for the Drude term in Eq. (1).

Figure 3 shows the optical conductivity $\sigma_1(\omega)$ at different T below 6000 cm^{-1}. There are two important features. One is the dramatic suppression of the spectral weight at low ω below 200 K. The lost spectral weight roughly shifts to the region between 2000 and 5000 cm^{-1}, leading to a very pronounced peak centered at 3200 cm^{-1} (0.4 eV). This is a clear indication of the formation of a gap in the charge excitation spectrum. The gap value can be roughly defined by the linear extrapolation of the peak edge, about 1250 cm^{-1} (0.15 eV) at lowest T. The second is the Drude-like response at both high and low T, if the very strong phonon contribution is subtracted. The conductivity value at the low frequency limit, which decreases as T decreases from 300 to 150 K but increases from 150 to 10 K, matches well the T-dependent behavior of the DC resistivity. A very narrow, sharp Drude component develops below the gap frequency in the CDW phase.

Previous experiments have not conclusively shown whether $1T$-$TiSe_2$ is a semiconductor with a very small energy gap or a semimetal with very low carrier density. As a bulk probe with very fine energy resolution, the present optical measurements reveal clearly that the compound is a semimetal with very low carrier density both above and below the CDW transition. Our data, in combination with results obtained from ARPES experiments, lead us to propose a schematic picture for the evolution of the electronic structure with T, displayed in Fig. 4. At room T, small numbers of Se $4p$ holes n_h and Ti $3d$ electrons n_e exist near Γ and L, respectively. Charge neutrality based on the stoichiometry of $1T$-$TiSe_2$ requires the same number of holes and electrons. This semimetallic picture, shown in Fig. 4(b), is in agreement with the band structure calculation by Zunger [5]. In this case, the plasma frequency reflects the contribution of two kinds of carriers with $\omega_p^2 = 4\pi e^2(\frac{n_h}{m_h} + \frac{n_e}{m_e})$, where m_h and m_e are the effective mass of p hole and d electrons, respectively.

On decreasing T from room temperature, the carrier density is expected to decrease due to the reduction of the thermally excited carriers for such a semimetal with small negative gap. This is the reason why the plasma edge shifts to lower ω. The increase of the DC resistivity in this temperature regime can be ascribed to this reduction of carrier numbers. An important consequence of the carrier number reduction is that the Coulomb interaction between electrons and holes becomes poorly screened. When the carrier density is low enough, the Coulomb interaction can lead to a bound state between an electron and a hole, i.e., an exciton. As a result, the free carriers are largely removed from the FS below 200 K.

Kohn and others have proposed an exciton driving mechanism for a CDW instability in a semiconductor or semimetal with a small indirect energy gap [22,23]. In the semimetal case, the electron-hole coupling acts to mix electron bands and hole bands that are connected by particular wave vectors which match the superlattice of CDW phase. The associated CDW transition, driven by the energy gain that arises from the gapping of the FS, is referred to as Overhauser type [22,24]. Considering charge neutrality, it appears that a direct mixing of the hole band near Γ and electron band near L can only lead to a hybridization gap at E_F, and thus an insulator in the CDW phase, in contradiction to experiments. $1T$-$TiSe_2$, however, appears to be a very special case. Because the ordering wave vector is commensurate, $2 \times 2 \times 2$, the new Brillouin zone is reduced in all three directions. Then, all the four points, Γ, A, L, and M shown in Fig. 4(a), become a new zone

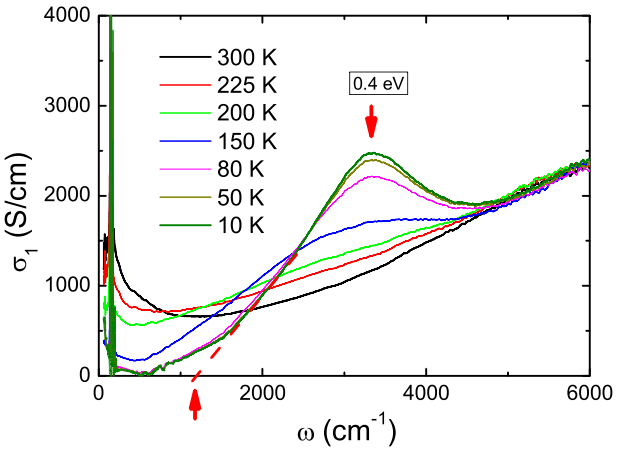

FIG. 3 (color online). Frequency dependence of the optical conductivity at different temperatures.

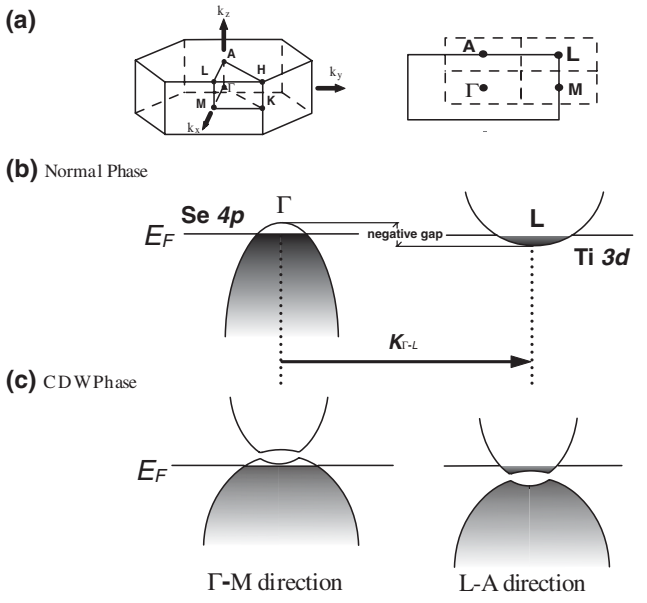

FIG. 4. Schematic picture for the evolution of the band structure with temperature. (a) The Brillouin zone layout for $1T$-$TiSe_2$. The right part shows the new Brillouin zones (dashed lines) for a $2 \times 2 \times 2$ superlattice in Γ, A, L , and M plane. (b) The semimetal picture in the normal phase. A small number of Se $4p$ holes and Ti $3d$ electrons exist near Γ and L, respectively. (c) The exciton state in the CDW phase caused by the Coulomb interaction between electrons and holes.

center of the $2 \times 2 \times 2$ superlattice. In this case, we need to consider all possible band mixing associated with the superlattice of the CDW phase. A band anisotropy can clearly be identified in the band structure calculations [5], which is an essential ingredient for such a semimetal-semimetal transition [22]. In addition to the hole and electron bands that cross E_F near Γ and L, respectively, the Ti $3d$ band near M is slightly higher than E_F, and the Se $4p$ band near A is slightly lower than E_F [5]. Apparently, the mixing of the band near M with that near Γ leads to a holelike subband (the split upper part of bands may not touch E_F), while the mixing of the band near A with that near L leads to an electronlike band [Fig. 4(c)]. Therefore, the compound enters into another semimetal state with a new balance of holes and electrons below the CDW transition. As indicated by Kohn, the new hole and electron bands have to be along different k directions. This is precisely what occurs for $1T$-$TiSe_2$. The above picture can explain very naturally the coexistence of the gap opening (due to the Γ-L band mixing) and metallic conduction in the CDW phase.

In the CDW state (below 200 K) the scattering of carriers is strongly reduced, leading to the rapid sharpening of the plasma edge in $R(\omega)$. The reduction of scattering can be attributed to the loss of a scattering channel by FS gapping. The sharp reduction of the conducting carrier density and the sharp reduction of carrier scattering leads to a peak in the DC resistivity near 150 K. Below 150 K, the carrier numbers do not further decrease, instead they increase slightly. The reduction of the DC resistivity on cooling below 150 K is dominated by the small and further decreasing carrier scattering rate.

The Overhauser-type CDW picture driven by strong electron-hole coupling appears to provide a good explanation for the variation of the DC and optical transport properties through the CDW transition in $1T$-$TiSe_2$. Excitons in semiconductors are a commonly observed phenomenon. However, such excitons are usually created by shining light on the semiconductor, which creates an equal number of electrons and holes. Such optically generated excitons have a very short lifetime, decaying quickly via the emission of light. The situation in $1T$-$TiSe_2$ is very different. It has an equal number of electrons and holes in $\boldsymbol{K}$ space in different bands. The very small carrier density leads to a stable formation of excitons at low T. $1T$-$TiSe_2$ might be the only real material for which the CDW transition is realized by the exciton condensation mechanism proposed by Kohn and others [22–24]. A closely analogous phenomenon is the Bose condensation of an electron-hole bound state (exciton) realized in connection with the quantum Hall effect observed in semiconducting bilayer systems [25].

To summarize, the optical measurements reveal that (i) $1T$-$TiSe_2$ is a semimetal with very low carrier density both above and below the CDW transition temperature; (ii) the carrier density changes with temperature, decreasing from room T to roughly 150 K, and then increases slightly with further decreasing T; (iii) an energy gap $\sim$0.15 eV develops below 200 K in the CDW phase; and (iv) dramatically different carrier scattering rates are present in the normal and CDW phases. The experimental data strongly suggest the presence of an Overhauser-type CDW transition in $1T$-$TiSe_2$. Further study will help us to understand why such an unusual CDW-bearing parent compound becomes a superconductor when a small percentage of excess electrons are doped into it via Cu intercalation.

We acknowledge very helpful discussions with W. Ku, T. M. Rice, T. Tohyama, R. S. Markiewicz, Z. Q. Wang, X. C. Xie, and Lu Yu. This work is supported by the National Science Foundation of China, the Knowledge Innovation Project of Chinese Academy of Sciences, and the Ministry of Science and Technology of China. M. Z. H. and R. J. C. acknowledge partial support through the NSF (No. DMR-0213706) and U.S. DOE Grants No. DE-FG-02-05ER46200 and No. DE-FG02-98ER45706.

*Corresponding author.
nlwang@aphy.iphy.ac.cn

[1] E. Morosan *et al.*, Nature Phys. **2**, 544 (2006).
[2] J. A. Wilson and A. D. Yoffe, Adv. Phys. **18**, 193 (1969).
[3] J. A. Wilson, F. J. Di Salvo, and S. Mahajan, Adv. Phys. **24**, 117 (1975).
[4] F. J. Di Salvo, D. E. Moncton, and J. V. Waszczak, Phys. Rev. B **14**, 4321 (1976).
[5] A. Zunger and A. J. Freeman, Phys. Rev. B **17**, 1839 (1978).
[6] R. Z. Bachrach, M. Skibowski, and F. C. Brown, Phys. Rev. Lett. **37**, 40 (1976).
[7] M. M. Traum *et al.*, Phys. Rev. B **17**, 1836 (1978).
[8] O. Anderson, R. Manzke, and M. Skibowski, Phys. Rev. Lett. **55**, 2188 (1985).
[9] Th. Pillo *et al.*, Phys. Rev. B **61**, 16 213 (2000).
[10] T. E. Kidd *et al.*, Phys. Rev. Lett. **88**, 226402 (2002).
[11] K. Rossnagel, L. Kipp, and M. Skibowski, Phys. Rev. B **65**, 235101 (2002).
[12] X. Y. Cui *et al.*, Phys. Rev. B **73**, 085111 (2006).
[13] D. Qian *et al.*, Phys. Rev. Lett. **98**, 117007 (2007).
[14] J. A. Wilson, Phys. Status Solidi B **86**, 11 (1978).
[15] C. S. Snow *et al.*, Phys. Rev. Lett. **91**, 136402 (2003).
[16] A. R. Beal, J. C. Knights, and W. Y. Liang, J. Phys. C **5**, 3531 (1972).
[17] J. A. Holy *et al.*, Phys. Rev. B **16**, 3628 (1977).
[18] H. P. Hughes and W. Y. Liang, J. Phys. C **10**, 1079 (1977).
[19] J. A. Wilson *et al.*, Phys. Rev. B **18**, 2866 (1978).
[20] S. C. Bayliss and W. Y. Liang, J. Phys. C **18**, 3327 (1985).
[21] E. Morosan, Lu Li, N. P. Ong, and R. J. Cava, Phys. Rev. B **75**, 104505 (2007).
[22] W. Kohn, Phys. Rev. Lett. **19**, 439 (1967).
[23] B. I. Halperin and T. M. Rice, Rev. Mod. Phys. **40**, 755 (1968), and references therein.
[24] A. W. Overhauser, Phys. Rev. Lett. **4**, 415 (1960).
[25] J. P. Eisenstein and A. H. MacDonald, Nature (London) **432**, 691 (2004).